

GA-A27414

EXPERIMENTAL DEMONSTRATION OF HIGH FREQUENCY ELM PACING BY PELLET INJECTION ON DIII-D AND EXTRAPOLATION TO ITER

by

**L.R. BAYLOR, N. COMMAUX, T.C. JERNIGAN, S.J. MEITNER, N.H. BROOKS,
S.K. COMBS, T.E. EVANS, M.E. FENSTERMACHER, C.J. LASNIER, R.A. MOYER,
T.H. OSBORNE, P.B. PARKS, E.J. STRAIT, E.A. UNTERBERG, and A. LOARTE**

OCTOBER 2012



DISCLAIMER

This report was prepared as an account of work sponsored by an agency of the United States Government. Neither the United States Government nor any agency thereof, nor any of their employees, makes any warranty, express or implied, or assumes any legal liability or responsibility for the accuracy, completeness, or usefulness of any information, apparatus, product, or process disclosed, or represents that its use would not infringe privately owned rights. Reference herein to any specific commercial product, process, or service by trade name, trademark, manufacturer, or otherwise, does not necessarily constitute or imply its endorsement, recommendation, or favoring by the United States Government or any agency thereof. The views and opinions of authors expressed herein do not necessarily state or reflect those of the United States Government or any agency thereof.

GA-A27414

EXPERIMENTAL DEMONSTRATION OF HIGH FREQUENCY ELM PACING BY PELLET INJECTION ON DIII-D AND EXTRAPOLATION TO ITER

by

**L.R. BAYLOR,* N. COMMAUX,* T.C. JERNIGAN,* S.J. MEITNER,* N.H. BROOKS,
S.K. COMBS,* T.E. EVANS, M.E. FENSTERMACHER,[†] C.J. LASNIER,[†] R.A. MOYER,[‡]
T.H. OSBORNE, P.B. PARKS, E.J. STRAIT, E.A. UNTERBERG,* and A. LOARTE[#]**

This is a preprint of a paper to be presented at the Twenty-fourth
IAEA Fusion Energy Conf., October 8-13, 2012 in San Diego,
California.

*Oak Ridge National Laboratory, Oak Ridge, Tennessee.

[†]Lawrence Livermore National Laboratory, Livermore, California.

[‡]ITER Organization, Cedex, France.

**Work supported in part by
the U.S. Department of Energy
under DE-AC05-00OR22725, DE-FC02-04ER54698,
DE-AC52-07NA27344, and DE-FG02-07ER54917**

**GENERAL ATOMICS PROJECT 30200
OCTOBER 2012**



Experimental Demonstration of High Frequency ELM Pacing by Pellet Injection on DIII-D and Extrapolation to ITER

L.R. Baylor 1), N. Commaux 1), T.C. Jernigan 1), S.J. Meitner 1), N.H. Brooks 2),
S.K. Combs 1), T.E. Evans 2), M.E. Fenstermacher 3), C.J. Lasnier 3), R.A. Moyer 4),
T.H. Osborne 2), P.B. Parks 2), E.J. Strait 2), E.A. Unterberg 1), and A. Loarte 5)

- 1) Oak Ridge National Laboratory, PO Box 2008, Oak Ridge, Tennessee 37831, USA
- 2) General Atomics, PO Box 85608, San Diego, California 92186-5608, USA
- 3) Lawrence Livermore National Laboratory, 7000 East Ave, Livermore, California 94550,
USA
- 4) University of California San Diego, 9500 Gilman Dr., La Jolla, California 92121-0417,
USA
- 5) ITER Organization, Route de Vinon sur Verdon – 13115 St. Paul lez Durance, France

e-mail contact of main author: BaylorLR@ornl.gov

Abstract. The injection of high repetition rate deuterium pellets is shown to trigger high-frequency edge localized modes (ELMs) in otherwise low natural ELM frequency H-mode deuterium discharges in the DIII-D tokamak. The resulting triggered ELMs have significantly lower energy and particle fluxes to the divertor than the natural ELMs. The plasma global energy confinement and density are not strongly affected by the pellet perturbations. The plasma core impurity density is strongly reduced with the application of the pellets. These experiments were performed in plasmas designed to match the ITER baseline configuration in shape and normalized β operation with input power just above the H-mode power threshold. This strongly reduced ELM intensity shows promise for exploitation in ITER to control ELM size while maintaining high plasma purity and performance.

1. Introduction

The high confinement mode (H-mode) of plasma operation is characterized by a steep pressure gradient and “pedestal” at the plasma edge, which leads to strong self-driven plasma currents that together result in an instability known as the edge-localized mode (ELM) [1]. ELMs expel periodic bursts of energy and particles from the plasma, which can pose a serious threat of plasma facing component (PFC) erosion and melting from the high heat fluxes and a source of impurities in the plasma. The intensity of ELMs must therefore be controlled in future large devices such as ITER.

High-frequency deuterium pellet injection experiments have been performed on the DIII-D tokamak to investigate the on-demand triggering of ELMs at rates much higher than the natural Type I ELM frequency to reduce the ELM intensity. This technique, known as pellet ELM pacing, has been proposed as a method to prevent large ELMs that can damage the ITER plasma facing components [2]. Previously, ELMs have been triggered on DIII-D using 1.8 mm pellets injected from low field side locations at rates up to 5 times the natural ELM rate [3], but ELMs in addition to those triggered by the pellets were observed indicating a change in the natural ELMing conditions. The pellet injector on DIII-D [4] has since been modified to produce smaller pellets (1.3 mm cylindrical size) and at much higher repetition rates with slower pellet speeds (<200 m/s) using new gas gun mechanisms. Experimental details of the pellet ELM pacing results and implications for ITER are reported here.

2. Pellet ELM Triggering Configuration

In these experiments, the pellets for on-demand ELM triggering were injected from the low field side (LFS) at the midplane (Fig. 1, MID) and at a newly installed lower port (Fig. 1,

R-2) that is similar to the injection geometry proposed for ITER. The LFS injection locations were chosen because of the higher sensitivity of these locations to trigger ELMs with pellets and low pellet fueling efficiency [5]. One barrel of the injector was connected to the midplane location while the other two barrels were connected to the lower X-point location. The nominal 1.3 mm pellet size contains 1.2×10^{20} atoms (2.4 mbar-L) of deuterium. Both injection trajectories lead to ELM triggering for this size and speed of pellet and no major difference is observed in the ELMs triggered from these locations. The flux expansion near the lower X-point enables a precise measurement of the position of the pellet in the plasma at the time of ELM onset for the X-point injected pellets. The ablation emission and magnetic loop measurements indicate that the pellets trigger ELMs when they reach the steep pressure gradient region of the edge pedestal.

A tangential viewing fast camera was available to image the injected pellets from both locations [6]. Fast camera images of the pellet entering the plasma from the LFS show the pellets becoming visible from ablation light just before the pellet reaches the separatrix. Near the separatrix (± 2 cm), a single plasma filament becomes visible just in front of the pellet cloud as shown in Fig. 2, similar to that observed previously for LFS vertically injected pellets [3]. The filament from the vertical pellets was observed to strike the outer vessel wall within 200 μ s of its formation. This is consistent with the hypothesis that the pellet cloud produces a local pressure perturbation that triggers a local ballooning mode instability that manifests itself as the reduced size ELM.

3. Pellet ELM Pacing Investigation

An investigation of ELM pacing was made by injecting the 1.3 mm cylindrical pellets at 60 Hz from the low field side into an ITER shaped plasma at $q_{95}=3.5$ with a low natural ELM frequency of 5 Hz, $\beta_N=1.8$, and normalized energy confinement factor $H_{98}=1.1$, with the input power only slightly above the H-mode threshold. The non-pellet similar discharges have ELM energy losses up to 55 kJ ($\sim 8\%$ of total stored energy), while the case with pellets demonstrated 60 Hz ELMs with an average ELM energy loss < 3 kJ ($< 0.5\%$ of the stored energy). Total divertor energy and peak heat flux from the ELMs is reduced on average by a factor greater than 10 as measured by an IR camera. Particle flux to the divertor from ELMs is also greatly reduced. Central impurity accumulation of Ni and other lower Z impurities is significantly reduced by the application of the 60 Hz pellets as shown in Fig. 3. No significant increase in density or decrease in energy

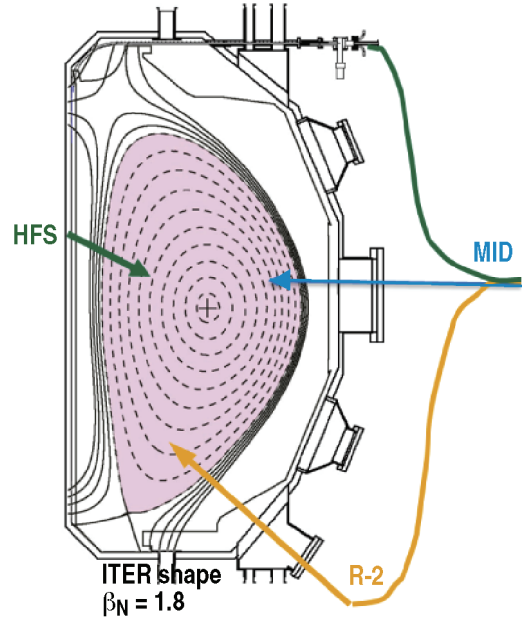


FIG. 1. Pellet injection geometry used for pellet ELM on demand triggering and fueling on DIII-D.

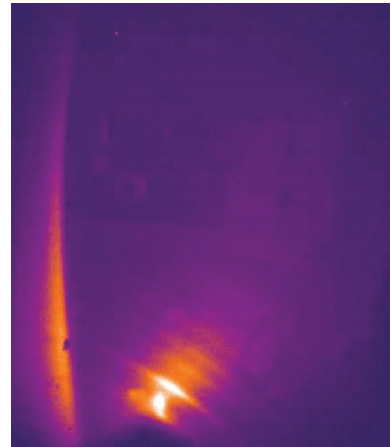


FIG. 2. Pellet injected from the R-2 location triggering a filament to be excited just in front of the pellet ablation cloud and subsequently forming an ELM.

confinement was observed with the pellets. The individual pellets are not observable in the interferometer density measurements due to their small size and that small ELMs are triggered within 0.5 ms of the pellet entering the plasma, ejecting the pellet mass.

The L-mode to H-mode transition in this plasma configuration occurs with a neutral beam power input of ~ 2.6 MW as has also been shown in earlier experiments with this configuration [7]. The neutral beam power was feedback controlled to maintain a constant $\beta_N = 1.8$, which resulted in a neutral beam power that averaged 2.8 MW. This is a modest 10% above the L-H threshold, similar to what ITER is expected to operate at. This typically results on DIII-D in a low type-I natural ELM frequency [7].

The plasma energy loss from each ELM in the two discharges determined from high time resolution divertor IR camera data [8,9] assuming toroidal symmetry is shown in Fig. 4. The pellet triggered ELMs have a more than 12x decrease in the average energy deposited in the divertor. The midplane pellet triggered ELMs have a factor of 2 lower average energy deposited per ELM than the X-point pellets. In the case of triggered ELMs, the ratio of energy deposited on the outer divertor compared to the inner divertor is $\approx 2.5:1$, while in the case of natural ELMs that ratio is $\approx 1:1$.

The divertor energy deposited and peak heat fluxes from ELMs were determined for a series of discharges with different pellet injection frequencies and without pellets. The results of this frequency scan are shown in Fig. 5. Both the total energy and peak heat flux show a trend of

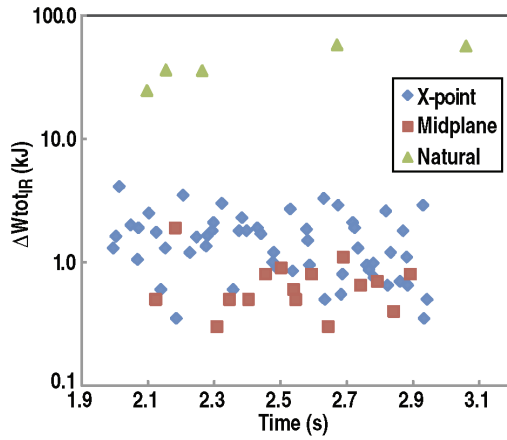


FIG. 4. Energy deposited (log scale) in the divertor from the IR camera data for each ELM in the discharges shown in Fig. 3. The natural ELMs are from the non-pellet comparison discharge.

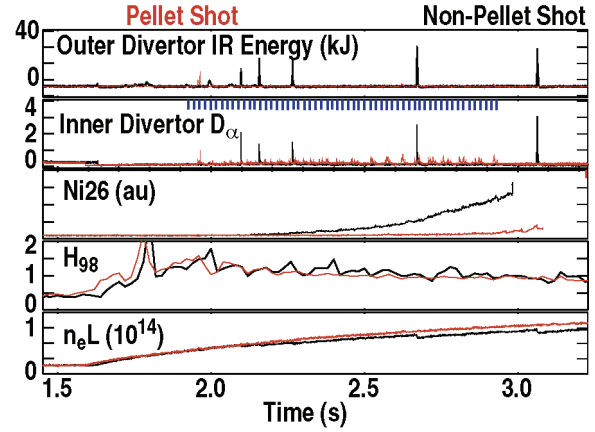


Fig. 3. Comparison of 60 Hz pellet case (red 147691) and no-pellet plasma with 5 Hz ELMs (black 147690). Divertor deposited energy and divertor particle flux are shown with nominal pellet times by blue tick marks. Central Ni emission, normalized energy confinement H_{98} , and electron density are shown.

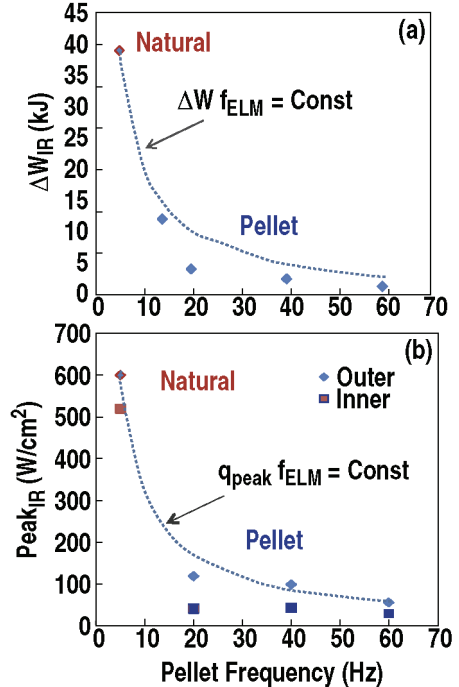


FIG. 5. Average density deposited in the divertor per ELM and peak heat flux as measured by the IR camera as a function of the pellet frequency.

reduced levels as a function of the pellet frequency. A curve showing the energy loss times ELM frequency equaling a constant is shown starting at the natural ELM frequency of 5 Hz. The data for the pellet triggered ELMs falls slightly under this curve. The peak heat flux on the outer strike point is found to be larger than on the inner strike point for all ELM frequencies including the 5 Hz natural ELMs [10].

All impurity emissivities measured by SPRED and CX show a reduced intensity with the application of high repetition rate pellet ELM triggering. Comparison of 20, 40, and 60 Hz pellets shows higher frequency reduces impurity levels more as seen in Fig. 6. These levels were measured at 0.8 seconds into the 1 s duration of the injection of pellets. After the pellets are stopped, the impurity emissivities increase to the non-pellet case levels within 0.3 s. The Ni impurity density in the core of the plasma has been modeled using the spectroscopic measurement of Ni XXVI 234 Å line intensity with the STRAHL impurity transport code [11] and is determined to be reduced by a factor of 3. Since n_e is not appreciably changed with the addition of pellets and T_e is not changed significantly, the emissivities of the high impurities are strongly indicative of changes in impurity density. For the lower Z impurities measured by CX, the emissivity is a direct measure of the impurity density. The reduction of impurities is hypothesized to be due to screening of the edge plasma by the enhanced particle flux stimulated by the rapid pellets and ELMs. High naturally occurring ELM rate plasmas with enhanced scrape off layer flows have been observed to have reduced impurity accumulation levels [12]. The lower injection frequencies of the pellets also result in reduced impurity content compared to the non-pellet reference plasma and the reduction in impurity density is found to increase linearly with the pellet repetition rate.

The electron density and temperature profiles for the two cases shown in Fig. 3 are shown in Fig. 7. The pellet case in this figure is broadly averaged over 200 ms (12 ELMs) independent of the ELM events. It can be seen that there is a reduced temperature pedestal width and height and a lack of profile stiffness when compared to the non-pellet case. The density profile is between the pre and post ELM profiles for the natural ELM case.

In the ITER shape discharges without pellet ELM pacing, Type I ELMs are believed to be caused by intermediate wavelength ($n \sim 3-30$) MHD instabilities that are driven by the sharp pressure gradient and bootstrap current across the edge barrier (pedestal). The ELMs are then triggered, and the pedestal pressure constrained, by the onset of Peeling-Ballooning modes [13]. A calculation of the peeling-balloonning stability of

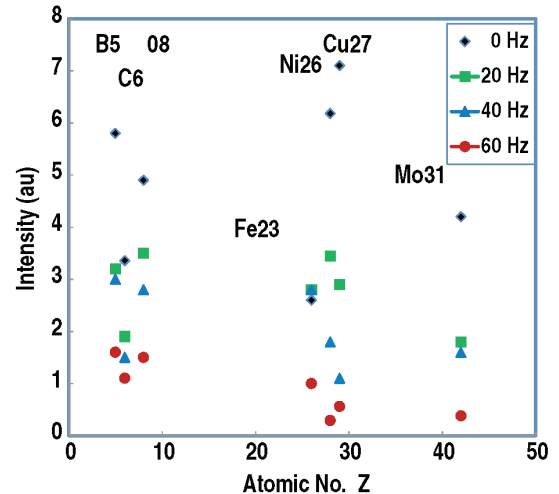


FIG. 6. Impurity intensity for natural and pellet triggered ELMs at different frequencies as a function of atomic number.

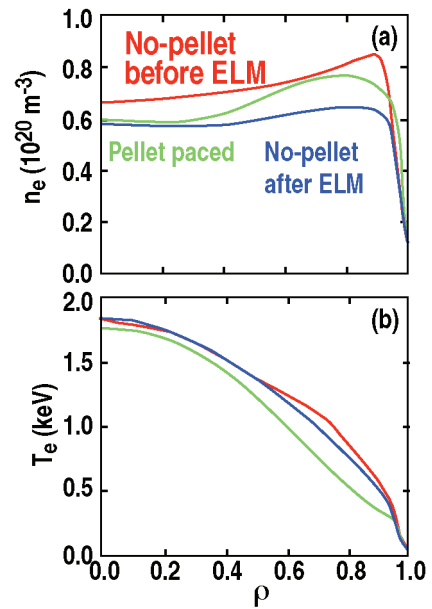


FIG. 7. Electron density and temperature profiles for the 60 Hz pellet case and natural ELM case before and just after a large ELM.

these discharges was made with the ELITE code [14–16] using equilibria based on the experimental pressure profiles from the measured temperatures and densities, broadly averaged over many ELM cycles independent of the ELMs for the pellet induced rapid ELM case. The results of this analysis are shown in Fig. 8 where the contours of maximum growth rate, normalized to the diamagnetic frequency, for intermediate n ($n=5\text{--}25$) are shown. In the natural ELMing case, the pedestal parameters are approaching the peeling unstable region just before a natural ELM crash (Pre) and are significantly removed from the unstable region just after an ELM crash (Post), consistent with this instability as the trigger for the ELMs. In the rapid pellet-triggered small ELM case, the pedestal conditions are well within the stable region. In the pellet pacing case (orange), a narrower pedestal width is observed that is consistent with a picture in which the pellets are triggering the ELMs before the width expands to the critical width at which the natural ELM occurs.

The pedestal total plasma pressure is reduced in the pellet ELM paced case to an average 6 kPa compared to a pedestal pressure of 11 kPa just before a natural ELM in the non-pellet comparison discharge and 7.5 kPa shortly after a natural ELM. This reduced pedestal height by the pellet ELM pacing is primarily in the electron pressure. Despite the reduction in pedestal electron pressure, the normalized confinement H98y2 [17] is not significantly affected. This is believed to be due to the profiles not remaining stiff when the pedestal electron temperature is reduced and to additional rotation shear that occurs when the pellets reduce the rotation at the plasma edge, while the central rotation is not reduced. The reduced impurity concentration also plays a role in maintaining the confinement when the pellets are applied. The edge Z_{eff} is reduced on the order of 50% based on the carbon reduction, which is the dominant impurity in these plasmas.

The pellet ablation emission data from the low field side R-2 injected pellets in DIII-D suggests that the ELM crash process begins when the pellet is just with ± 2 cm of the pellet crossing the separatrix along the R-2 trajectory. This is a somewhat shallower triggering location than was observed on ASDEX-Upgrade [2] and JET [18] with pellets injected from the high field side (inner wall). The top of the edge pedestal at the R-2 X-point injection location on DIII-D is >4 cm inside of the separatrix because of flux expansion that occurs near the divertor. The pedestal top at the midplane is <2 cm inside the separatrix making resolution of the pellet location there when an ELM is triggered more difficult. This R-2 ELM triggering result implies that the ITER requirement for low field side injected ELM pacing pellets to reach the top of the pedestal may be overly conservative. Future studies with even smaller pellets are planned to elucidate just how far inside the separatrix the pellets need to penetrate and how much mass is necessary. The filaments that are released during the ELM crash triggered by the pellet are observed to hit the wall locally near the pellet injection location. While most of the stored energy loss can be accounted for by extrapolating the heat

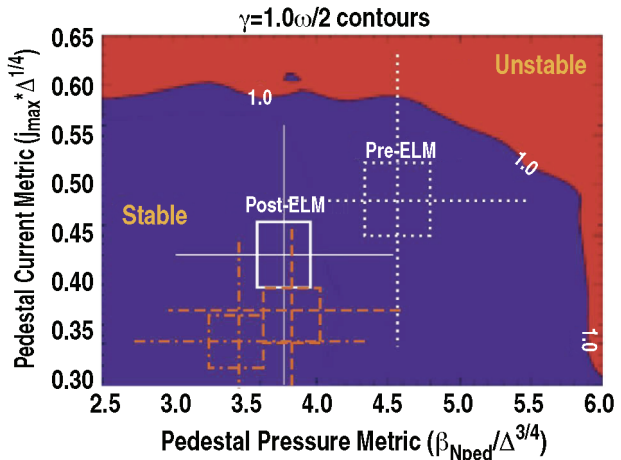


FIG. 8. Normalized shear plotted against normalized pressure for the pedestal location on these pellet (147691-orange) and non-pellet (147690-white) comparison discharges in Fig. 2. ELITE calculation of the boundary for peeling and ballooning stability is shown for this plasma configuration.

flux measured in the divertor by the IR camera, it is clear that some level of heat flux from the pellet triggered ELM, yet to be quantified, may impinge on the outer wall.

One potential result of triggering the ELMs locally by pellets is a possible non-axisymmetric heat flux on the divertor plasma facing components. This could be induced by a local ELM filament generated in the vicinity of where the pellet pressure perturbation interacts with the pedestal, which is observed on DIII-D by fast camera imaging. Since the axial heat flux along such a filament is much greater than any radial conducted flux [19], it would be expected that the majority of the heat flux deposited by such a filament would occur where the filament strikes the divertor. This picture is consistent with observations of the divertor heat flux from pellet triggered ELMs in JET [18,20] that show the divertor footprint is not completely axisymmetric and is a function of the edge safety factor.

4. ITER Extrapolation

The ELM pacing experiments on DIII-D were performed in conditions as closely matching those expected on ITER as is possible, with a similar shaped plasma (Fig. 9) and normalized β . Some of the parameters such as magnetic field (B_ϕ), normalized gyro radius (ρ^*) are not physically realizable on DIII-D or any other present day tokamak, making a direct comparison with ITER projections impossible. One of the important parameters where there is good comparison to ITER is the applied power relative to the H-mode threshold power. It is anticipated that ITER will operate marginally above the H-mode power threshold [17]. This DIII-D experiment was performed with a NBI power that was $\sim 10\%$ above the H-mode power threshold for this plasma shape and current, which is one reason for the extremely low natural ELM frequency of ~ 5 Hz. Since ITER is also expected to operate marginally above the H-mode threshold, it will likely have a low natural ELM frequency and thus will need ELMs to be triggered in the 10–60 Hz range to control the confined plasma tungsten concentration and/or keep the divertor heat flux to a manageable level. The DIII-D ELM pacing frequency multiplier of 12 and resulting reduction of divertor heat flux achieved by the same factor in this experiment is approaching that desired for ITER.

More recent experiments on DIII-D have been performed to investigate the triggering of ELMs with smaller pellets for better extrapolation to ITER and combining pellet ELM pacing with fueling from high field side (HFS) pellet injection. The pellet size was reduced by 40% by changing the extruder nozzle to produce thinner solid D₂ extrusions. The resulting pellets were found to reliably trigger ELMs from both low field side injection locations and thus the minimum pellet size and penetration to trigger an ELM has yet to be determined. The full size 1.3 mm pellets were injected from the HFS location shown in Fig. 1 in ITER shape plasmas to investigate fueling in ITER like operating scenarios in combination with LFS pellet ELM pacing. The HFS pellets were found to also trigger ELMs like the LFS pellets, but a strong difference in the density perturbation was observed. HFS pellets were injected at up to 20 Hz and resulted in a significant density increase compared to non-pellet or LFS only

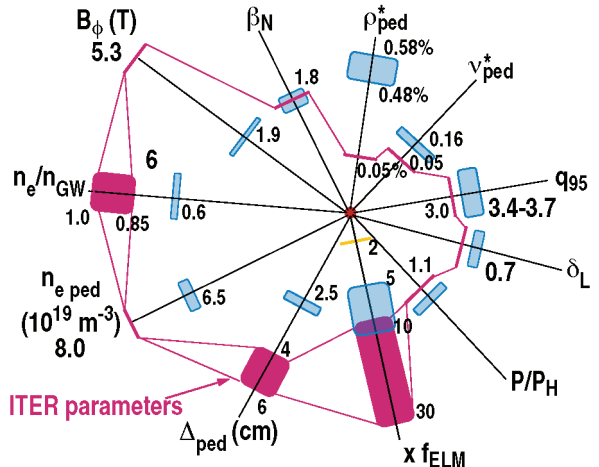


FIG. 9. Multi-parameter star plot showing the DIII-D pellet ELM pacing parameters (blue) compared to predicted ITER parameters (magenta).

pellet injection cases. No significant reduction in plasma confinement was observed when the HFS pellets were applied.

Important remaining issues that need to be addressed regarding the application of this technique to ITER include: the required pellet size to reliably trigger ELMs (which has implications for the fuel throughput and pumping needed), the adequacy of the ITER pellet injection geometry (in the low field side of the plasma above the X-point) for ELM triggering with the available pellet speeds, and possible toroidal asymmetries of divertor power for pellet triggered ELMs [21]. Modeling of ELM triggering by pellet injection has been performed with the nonlinear MHD code JOREK, which has been upgraded to include an appropriate description of the pellet ablation physics [22]. Predictions have been compared with these experiments in DIII-D in which ELMs have been triggered by injection of pellets at the MID and R-2 locations. The JOREK simulations show that triggering of ELMs by pellet injection is caused by the large toroidally-localized edge pressure gradients produced by the ablating pellet. When these gradients exceed a threshold, ballooning modes grow nonlinearly leading to the ELM crash [23]. Exceeding this pressure gradient threshold implies that, for given pedestal plasma conditions, a minimum pellet size is required to trigger an ELM. JOREK modeling shows that this minimum pellet size depends on the injection geometry and that for injection above the X-point the required pellet size in DIII-D is a factor of ~ 2 smaller than for midplane injection. This implies that the ITER pellet injection geometry for ELM triggering is advantageous to reduce the fuel throughput requirements associated with this ELM control scheme. Modeling of the divertor power flux for pellet triggered ELMs in DIII-D shows that this has a sizeable non-toroidally symmetric peak (i.e. of similar magnitude to the separatrix strike point ELM power flux) away from the separatrix at the outer divertor, which has also been observed at JET [20]. Future experiments on DIII-D will be aimed at trying to quantify the level of non-axisymmetric heat flux arising from the pellet induced ELMs using a new periscope providing a tangential view of the divertor in infrared.

5. Summary

Low field side injected pellets in DIII-D have been found to greatly reduce the ELM intensity and simultaneously greatly reduce impurity accumulation when applied at rates in excess of 10x the natural ELM rate. The pedestal height and width are reduced by the pellet ELM pacing while not appreciably affecting plasma confinement, all of which are promising for ITER. The triggering of the ELMs takes place well before the pellet reaches the top of the pedestal, implying that even smaller pellets may be utilized. Future studies with smaller pellets will elucidate just how far inside the separatrix the pellets need to penetrate. Further optimization and extension to even higher frequency smaller pellet ELM pacing is needed to fully explore and extrapolate this ELM mitigation technique to ITER.

In summary, the triggering on demand of ELMs by injecting small pellets at a rate of 12X the natural ELM event rate with a strong reduction ($>12X$) in ELM heat flux has been observed in DIII-D H-mode plasmas. Both the inner and outer legs of the divertor are found to have a reduced heat flux. This result was facilitated by the injection of small 1.3 mm pellets at <200 m/s from the low field side near the X-point where the pellets are able to trigger ELMs reliably deposit no fuel into the plasma. The small pellet induced ELMs are able to keep the plasma pedestal width from expanding to the critical width at which the large natural ELMs occur. Continued optimization of the pellet size and frequency are needed to further reduce the triggered ELM intensity in a steady-state operating scenario.

This work was supported by the Oak Ridge National Laboratory managed by UT-Battelle, LLC for the US Department of Energy under DE-AC05-00OR22725; and the US Department of Energy under DE-FC02-04ER54698, DE-AC52-07NA27344, and DE-FG02-07ER54917. The views and opinions expressed herein do not necessarily reflect those of the ITER Organization. The authors also thank S.L. Milora, J.H. Harris, P.T. Lang, and T.S. Taylor for enlightening discussions and support and the DIII-D team for operating the experiment.

References

- [1] ZOHM, H., Plasma Phys. Controlled Fusion **38** (1996) 105
- [2] LANG, P.T., et al., Nucl Fusion **44** (2004) 665
- [3] BAYLOR, L.R., et al., Proc. 37th EPS Conf. on Controlled Fusion and Plasma Physics (Dublin, Ireland) P2.117; <http://ocs.ciemat.es/EPS2010PAP/pdf/P2.117.pdf>
- [4] COMBS, S.K., et al., J. Vac. Sci. Tech. **A6** (1988) 1901
- [5] BAYLOR, L.R., et al., Nucl. Fusion **47** (2007) 1598
- [6] YU, J.H., et al., Phys. Plasmas **15** (2008) 032504 (2008)
- [7] DOYLE, E.J., et al., Nucl. Fusion **50** (2010) 075005
- [8] HILL, D.N., et al., Rev. Sci. Instrum. **59** (1988) 1878
- [9] HERMANN, A., J. Nucl. Mater. **337–339** (2005) 907
- [10] LOARTE, A., IAEA 2010
- [11] BEHRINGER, K., “Description of the impurity transport code STRAHL, Jet Joint Undertaking Document JET-R (87)08 (Culham: JET Joint Undertaking) (1987)
- [12] WADE, M.R., et al., J. Nucl. Mater. **44–50** (1999) 266
- [13] SNYDER, P.B., et al., Phys. Plasmas **9** (2002) 2037
- [14] WILSON, H.R., et al., Phys. Plasmas **9** (2002) 1277
- [15] SNYDER, P.B., et al., Nucl. Fusion **47** (2007) 961
- [16] SNYDER, P.B., et al., Phys. Plasmas **19** (2012) 056115
- [17] ITER Physics Expert Group on Confinement Modeling, Database, and ITER Physics Basis Editors 1999 Chapter 2: Plasma confinement and transport, Nucl. Fusion **39** (1999) 302
- [18] LANG, P.T., et al., Nucl. Fusion **51** (2011) 033010
- [19] BOEDO, J.A., et al., Phys. Plasmas **12** (2005) 072516
- [20] WENNINGER, R.P., et al., Nucl. Fusion **53** (2011) 105002
- [21] LOARTE, A., et al., paper ITR/P1-2, this conference
- [22] HUIJSMANS, G., et al., paper ITR/P1-23, this conference
- [23] FUTUTANI, S., et al., paper ITR/P1-22, this conference